

The high strain rate compressive behaviour of polycarbonate and polyvinylidene difluoride

C.R. Siviour*, S.M. Walley, W.G. Proud, J.E. Field

PCS Group, Cavendish Laboratory, Department of Physics, University of Cambridge, Madingley Road, Cambridge CB3 0HE, UK

Received 8 June 2005; accepted 25 October 2005

Available online 11 November 2005

Abstract

Measurements are presented of the compressive stress–strain behaviour of polycarbonate (PC) and polyvinylidene difluoride (PVDF) at strain rates from 10^{-4} to 10^4 s^{-1} at room temperature, and temperatures from -50 to $+150 \text{ °C}$ at 10^3 s^{-1} . These results, obtained using a split Hopkinson pressure bar and Instron testing machine, are supported by dynamic mechanical analysis (DMA) measurements on the materials. Previous researchers have observed that the yield stress of these materials is bilinearly dependent on the logarithm of strain rate. The data presented here show that the bilinearity is due to the movement of low order transitions in the materials, so that they occur at temperatures above room temperature at the higher strain rates. In particular, these transitions are the β transition in PC, and the glass transition in PVDF. In addition, Appendix A presents measurements of a high strain rate Poisson's ratio of polycarbonate and its evolution with strain.

© 2005 Elsevier Ltd. All rights reserved.

Keywords: Split Hopkinson pressure bar; Polycarbonate; Polyvinylidene difluoride

1. Introduction

The mechanical properties of polymers are of great scientific and industrial importance. A huge volume of literature exists on properties at different temperatures, strains and strain rates, and in different modes of loading. However, there is relatively little published work on their mechanical properties at high (above 1 s^{-1}) strain rates. The aim of the experiments reported here was therefore twofold. Firstly, to provide reliable and complete data for constitutive model development, and secondly, to understand the changes in behaviour that occur at high strain rates. In particular, it has been observed for some polymers that the dependence of yield stress on strain rate is greater at high rates. It will be shown that this can be explained in terms of molecular transitions in two polymers: polycarbonate (PC) and polyvinylidene difluoride (PVDF).

The first study of the stress–strain behaviour of polymers over a wide range of strain rates is usually regarded as being that of Chou et al., who examined the behaviour of polymethyl methacrylate (PMMA), cellulose acetate butyrate,

polypropylene and nylon 66, in compression, using a 'medium strain-rate machine' and a split Hopkinson pressure bar (SHPB) [1]. In particular, he plotted the mechanical strength of these materials as a function of strain rate. Whilst it was expected that the stress supported at a given strain would be a linear function of $\log(\dot{\epsilon})$, where $\dot{\epsilon}$ is the strain rate, it was in fact found that at high rates this stress increased more quickly. An increase in the strain rate dependence of yield stress was also observed by Briscoe and Hutchings [2] and Kukureka and Hutchings [3] for high density polyethylene (HDPE). However, doubt was cast on the validity of the measurements [1–3] by Briscoe and Nosker, who considered carefully the effects of friction and specimen response in the Hopkinson bar [4,5]. They concluded that in fact the yield strength of HDPE is linear in $\log(\dot{\epsilon})$. Gorham suggested that inertia might be the cause of a similar observed effect in copper [6].

Walley and Field [7–9] examined the behaviour of a large number of polymers, at room temperature, over strain rates ranging from 10^{-2} to 10^4 s^{-1} , taking great care to use suitable lubrication and specimen sizes to reduce friction and inertia. Again, they plotted the yield stress as a function of $\log(\dot{\epsilon})$, and found that the different materials fell into three different groups:

- A linear relationship, with no change at higher strain rates.
- A bilinear behaviour with a sharp increase in gradient at a strain rate of $\sim 10^3 \text{ s}^{-1}$.

* Corresponding author. Tel.: +44 1865 283473; fax: +44 1865 273813.

E-mail address: clive.sivions@eng.ox.ac.uk (C.R. Siviour).

- A decrease in maximum stress at a strain rate of $\sim 10^3 \text{ s}^{-1}$, possibly followed by an increase.

In particular, HDPE fell into the linear group, whilst polypropylene showed a bilinear dependence. Therefore, the observations of Briscoe and Nosker and those of Chou are not incompatible. The unexpected result in the work of Walley and Field was the decrease in strength of some polymers at high strain rates: nylon 66, polycarbonate (PC), polyetheretherketone (PEEK) and polyethersulphone (PES). Nylon 66 and PC had been part of the Chou study, and PC was also investigated over a range of strain rates and temperatures by Rietsch and Bouette [10] and over a range of strain rates by Bisilliat et al. [11]. None of these studies observed a decrease in strength; however, this may be because they did not go to high enough strain rates for the grade of polymer that they used.

Drops in yield stress for PEEK and nylon 66 at high strain rates were confirmed by Al-Maliky et al. [12]. In addition, they and Hamdan and Swallowe [13,14] found that in both cases the drop was preceded by bilinear behaviour. The steeper part of the bilinear relationship occurred over too small a range of strain rates to have been observed by Walley and Field. This confirmed that the drop in strength observed by Walley and Field was not inconsistent with the bilinear behaviour in other studies on the same materials. In addition, use of the expanding ring technique showed that this behaviour is not only observed in Hopkinson bar experiments [15].

The cause of this behaviour is still not established. In fact, some authors doubt whether it is a true material property. For example, Diah et al. attributed it to specimen size effects in the Hopkinson bar, and present results that show the effect is reduced for smaller specimen thicknesses [16,17]. Hamdan and Swallowe [13], Al-Maliky et al. [12] and Swallowe and Fernandez [18,19] suggested that the behaviour was due to an increase in crystallinity occurring during deformation. However, Swallowe and Lee [20] showed that for PET this increase develops too late in the deformation to contribute to the yield and flow stress. Instead they suggested that activation volume changes may play a role.

As well as strain rate, temperature has an important effect on the mechanical properties of polymers. Bauwens-Crowet conducted a series of compression experiments on PMMA at rates between 10^{-4} and 10^0 s^{-1} [21]. Each of these rate sweeps was repeated every 20°C between -20 and 100°C . The dependence of yield stress on strain rate and temperature was reported, and using a time–temperature superposition they extended the range of the experiments to 10^{+6} s^{-1} at 100°C . In addition, the material was tested at a strain rate of $4 \times 10^{+3} \text{ s}^{-1}$ over a range of temperatures. Both sets of data showed a bilinear relationship, with increased strength at high strain rates and at low temperatures. In earlier papers, Bauwens and colleagues had investigated PC in compression over a range of temperatures, and found a similar relationship [22,23]. This behaviour was attributed to the different molecular relaxations in the material. At high temperatures or low strain rates only the α relaxation (glass transition) plays a role in the polymer behaviour, whilst at low temperatures

and high strain rates, the effect of the β relaxation is added to that of the α . The authors developed a model to explain the behaviour, and this was also used by Rietsch and Bouette [10]. An advantage of the Bauwens and Bauwens-Crowet experiments is that they were performed in the same apparatus, and effects such as inertia and specimen equilibrium could be ignored. However, their explanation may not apply to all polymers: Swallowe and Lee observed that the β relaxation in PMMA and PS merges into the α at rates above 1 s^{-1} [20]. Despite this, the approach of Bauwens and Bauwens-Crowet, to examine the effect of both strain rate and temperature, is used in the research presented here.

An important piece of information from the work of Chou et al. [1] was their measurements of temperature rises in the specimens as they deformed. In particular, the temperature rise was very small at low strains, but increased dramatically after yield. This result, which is also seen in the work of Rittel [24], will be considered in Appendix A.

2. Experimental overview

2.1. Choice of materials

Two materials were investigated: PC and PVDF. PC is an amorphous polymer with a glass transition temperature above room temperature, PVDF is a semi-crystalline polymer whose glass transition temperature is below room temperature. These materials were chosen because, in the study by Walley and Field, they exhibited different behaviour from each other. The yield stress of PC was linearly dependent on $\log(\dot{\epsilon})$ over the low strain rate region, but dropped at high strain rates (although this was not observed by Rietsch and Bouette). That of PVDF had a bilinear dependence on $\log(\dot{\epsilon})$.

The structure of bisphenol-A polycarbonate, the type used in this study, is shown in Fig. 1. It is an amorphous polymer with a glass transition temperature (T_g) of the order 148°C , and a beta relaxation temperature (T_β) of the order -60°C . The structure of PVDF is shown in Fig. 2. This is a crystalline

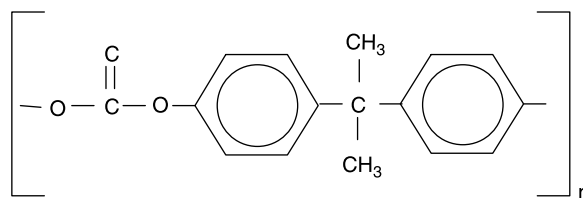


Fig. 1. The structure of bisphenol-A-polycarbonate.

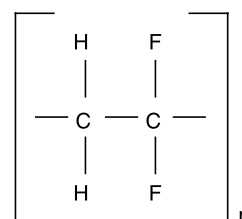


Fig. 2. The structure of polyvinylidene difluoride.

polymer, with three crystalline forms (or phases) designated α , β and γ . The form that is obtained in a given specimen depends on its preparation; however, the annealing process used in these experiments was designed to give a stable structure consisting of spherulites of α -phase in addition to some amorphous material. This annealing regime is given in Section 4.1. Fig. 2 shows that the monomer is not symmetrical, and two monomers can either be joined ‘head-to-head’, or ‘head-to-tail’. The glass transition of PVDF is at approximately $-30\text{ }^{\circ}\text{C}$, and the melting point is given by the manufacturer as $174\text{ }^{\circ}\text{C}$.

2.2. Experimental design

A weakness of the experimental studies discussed in Section 1 was that two different types of apparatus were used: usually an Instron mechanical testing machine at low strain rates (up to 1 s^{-1}), and a split Hopkinson pressure bar (SHPB, [25,26]) at high rates (10^2 – 10^5 s^{-1}). Unfortunately, the bilinearity in material behaviour was observed to occur at the same strain rate as the change of apparatus.

In this study, experiments were performed over both a range of temperatures in the SHPB, and a range of strain rates using an SHPB and an Instron machine. This allowed material changes to be isolated from those imposed by the experimental apparatus. Specimen sizes were chosen to limit the effect of inertia at high rates [27], and paraffin wax was used as a lubricant [7,8]. Since any effects due to the experimental technique would be the same for all the SHPB experiments, any changes in strength with temperature can be related to material properties. Using a time–temperature mapping, similar to the well-known WLF formula [28], these were then compared to those changes that occurred with strain rate.

By comparing these results with dynamic mechanical analyser (DMA) tests on the materials in question, the dependence of the yield stress on both strain rate and temperature was linked to the relaxations in the materials. In this research, the DMA testing was performed in a single cantilever arrangement.

3. Polycarbonate

3.1. Material and specimen preparation

The PC used was Bayer Makrolon[®] 2805. This consists of bisphenol-A PC mixed with a mould release additive, and is described as a medium viscosity grade of PC. Some properties obtained from the manufacturer’s data sheet are shown in Table 1. The compression specimens were injection moulded into discs of various sizes. In addition, there were some injection-moulded cylinders from which specimens were cut for DMA tests. All specimens were annealed according to the manufacturer’s instructions: hold at $125\text{ }^{\circ}\text{C}$ for 30 min and then cool slowly to room temperature.

Table 1
Selected properties of Makrolon[®] 2805

Glass transition temperature	ca. $145\text{ }^{\circ}\text{C}$
Density	1.2 g cm^{-3}
Coefficient of linear thermal expansion	$6.0 \times 10^{-5}\text{ mm}^{-1}\text{ }^{\circ}\text{C}^{-1}$
Tensile modulus	2.4 GPa
Tensile strength at yield	65 MPa
Tensile strength at break	70 MPa
Compressive strength at yield	76 MPa
Poisson’s ratio	0.4
Specific heat	$1172\text{ J kg}^{-1}\text{ K}^{-1}$
Melt flow rate at $300\text{ }^{\circ}\text{C}/1.2\text{ kg load}$	10 g/10 min

All at room temperature.

3.2. Experimental conditions

Hopkinson bar experiments were performed at room temperature over the strain rate range 10^3 – 10^5 s^{-1} , and at ca. 5500 s^{-1} over the temperature range -60 to $+175\text{ }^{\circ}\text{C}$. All the specimens were 5 mm in diameter and two thicknesses were used: 0.75 and 1.5 mm. Generally the thinner specimens were used at higher strain rates, although it was found that there was no discernible difference between results from the two specimen lengths. At 10^5 s^{-1} , the inertial contribution to the measured flow stress for a 1.5 mm long specimen is 92 kPa, and for a 0.75 mm long specimen is 58 kPa [27]. These values are negligible compared to the room temperature flow stress of PC at this rate: $\sim 120\text{ MPa}$. Since the specimens have a large diameter/length ratio, lubrication could be a concern; however, it is well established that paraffin wax provides essentially perfect lubrication over all temperatures down to at least $-60\text{ }^{\circ}\text{C}$ [29]. Specimen equilibrium was also confirmed by comparing the one-wave and two-wave analyses for specimens stress.

Some measurements of the high strain rate Poisson’s ratio were performed during the room temperature experiments, these are presented in the Appendix A. Instron experiments were carried out at strain rates between 10^{-4} and 10^0 s^{-1} at room temperature. DMA analysis was performed at 1, 10 and 100 Hz between -100 and $200\text{ }^{\circ}\text{C}$.

3.3. Results

This research produced a large number of stress–strain curves. A representative selection of these will initially be presented in full, and, in the discussion, all the data collected will be parameterised for comparison between different strain rates and temperatures.

Fig. 3 shows stress–strain curves for PC over a range of strain rates. All of these specimens exhibited an elastic response up to a strain of approximately 0.1, where they yielded. The yield stress is a function of strain rate, and in the SHPB ranges from about 110 MPa at 2240 s^{-1} to about 120 MPa at $10,280\text{ s}^{-1}$. After yield, there is some strain softening to a strain of 0.3 after which the material strain-hardens again. Because of the nature of the loading apparatus each specimen is loaded for a fixed length of time, approximately 80 μs . This means that the strains achieved

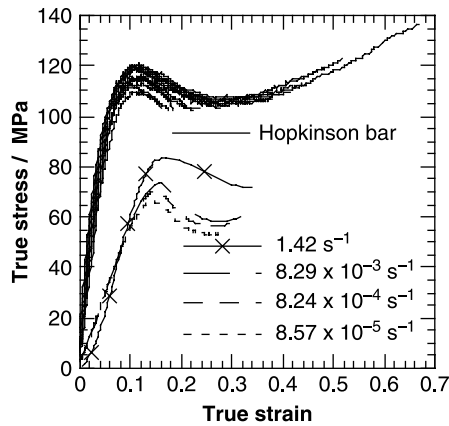


Fig. 3. Room temperature (21 °C) stress–strain curves for PC specimens. Hopkinson bar strain rates range from 2240 to 10,280 s^{-1} .

were higher in the experiments at higher strain rates. In all cases, the end of the stress–strain curve represents the end of the experiment, and is not related to any material property. In addition, all strain rates quoted are true strain rates, and are accurate to better than $\pm 1\%$. The Instron data show similar features, with lower stresses reflecting the lower strain rates applied.

SHPB experiments were also performed over a range of temperatures between -60 and 175 °C, at a strain rate of $5500 \pm 500 s^{-1}$; stress–strain curves are shown in Fig. 4. The yield and flow stresses increase with decreasing temperature, as does the strain at yield. The experiment at 175 °C shows the effect of the glass transition temperature, which is higher than the value of 145 °C quoted by the manufacturer because of the high strain rate. An interesting feature of this experiment was the formation of voids in the specimen. The density of the material, measured using Archimede's method, decreased from $1.19 \pm 0.01 g cm^{-3}$ before the experiment to $1.03 \pm 0.01 g cm^{-3}$ afterwards. The same voiding and density change was observed in the specimen used for the DMA tests.

Finally, DMA was performed (Fig. 5). The DMA data show the effects of three different relaxations. The drop in modulus at ~ 150 °C is associated with the glass transition temperature,

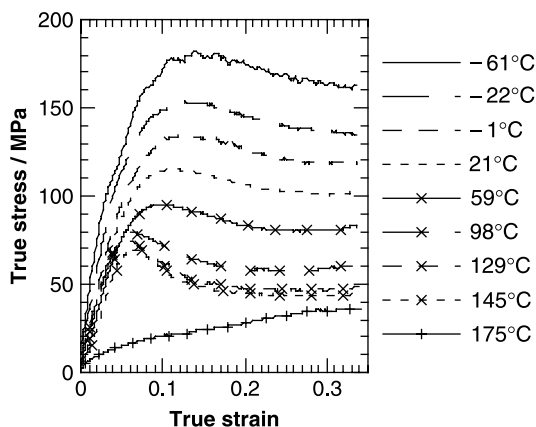


Fig. 4. Hopkinson bar stress–strain curves for specimens of PC over a range of temperatures. The strain rate was $5500 \pm 500 s^{-1}$.

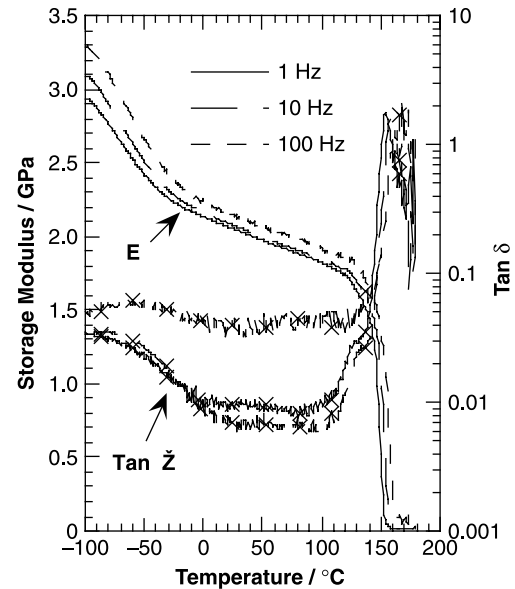


Fig. 5. Storage modulus and $\tan \delta$ for PC at frequencies of 1, 10 and 100 Hz, over temperatures from -100 to 180 °C in a single cantilever configuration. The strain amplitude was $0.030 \pm 0.001\%$ and the equivalent strain rates are therefore $6 \pm 0.2 \times 10^{-4}$, 6×10^{-3} and $6 \times 10^{-2} s^{-1}$. The data at 100 Hz do not appear to be as good as those at 1 and 10 Hz, this is thought to be due to the machine not being so accurate at the high frequency. Note that the loss tangent is shown on a logarithmic axis.

and the increase below -30 °C with the β transition. The molecular origins of these relaxations are not well-established [30].

3.4. Discussion of experimental results

This discussion shows that the compressive stress–strain curves at different strain rates can be related to those at different temperatures via a one parameter mapping that relates temperature to $\log(\dot{\epsilon})$. This is used to map all of the data to a strain rate of $5500 s^{-1}$, and confirmation of the validity of the mapping is provided by applying it to stress–strain curves from the literature. Next, the DMA curves are used to consider the dependence of the glass and beta transition temperatures on strain rate. It is shown that the observed glass transition temperature at $5500 s^{-1}$ is consistent with that extrapolated from the DMA data, and the upper temperature of the β transition region at this strain rate is calculated to be approximately 40 °C. This temperature is consistent with that at which the dependence of yield strain on temperature and strain rate changes. Therefore, it is concluded that the increase in strength of PC at high strain rates is due to the β transition temperature being above room temperature at these rates.

3.4.1. Compressive stress–strain curves

Having presented the full stress–strain curves, the data will now be reduced to a single parameter—peak stress at yield—for comparison. Fig. 6 shows a plot of peak stress against $\log(\dot{\epsilon})$ and Fig. 7, peak stress against temperature. It should be noted that the strain rate dependence is not the same as that observed by Walley and Field [9]. This is discussed in Section 5.

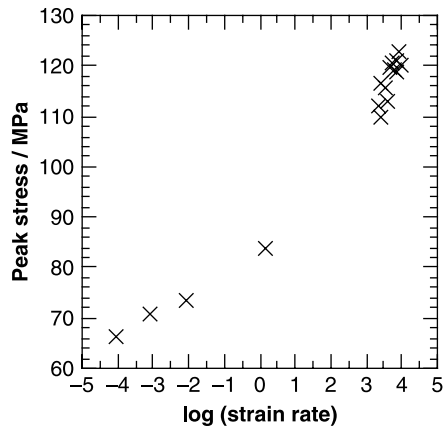


Fig. 6. Plot of maximum stress against strain rate at 21 °C, showing the two distinct regions in the data.

A mapping was developed to relate temperature to strain rate for these data using a simple formula with one parameter, A :

$$T = T_0 + A(\log \dot{\epsilon}_0 - \log \dot{\epsilon}). \quad (1)$$

From measurements taken during the room temperature experiments T_0 was 21 °C. The nominal strain rate of the Hopkinson bar experiments over a range of temperatures was 5500 s^{-1} , so this was chosen as $\dot{\epsilon}_0$. The results of this mapping are shown in Fig. 8, using $A = 17 \text{ K}$. It is important to note that the mapping is valid because in Eq. (1) there is only one variable parameter whereas there were two different gradients in the dependence of maximum stress on strain rate.

Further confirmation of the mapping was provided by data from the literature. Blumenthal et al. measured compressive stress–strain curves of PC [31]; whilst they investigated fewer temperatures and strain rates than this study, data were presented from low strain rate experiments at different temperatures. Their experimental conditions, and the peak stress under each condition, are summarised in Table 2. These data were mapped to 2000 s^{-1} , using $A = 17 \text{ K}$, but this time with T_0 as the temperature of the experiment, and $\dot{\epsilon}_0 = 2000 \text{ s}^{-1}$. Although Blumenthal et al. do not state which grade of PC was used, a comparison with the experiments

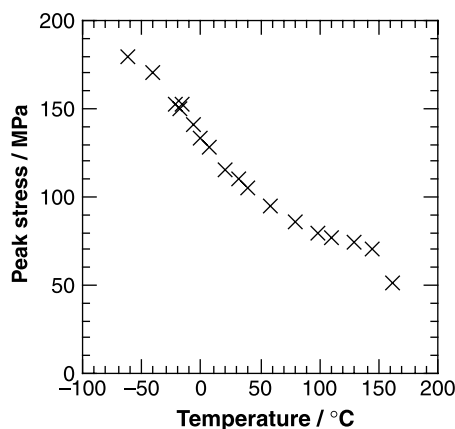


Fig. 7. Plot of maximum stress against temperature at $5500 \pm 500 \text{ s}^{-1}$. The result at 175 °C is not shown.

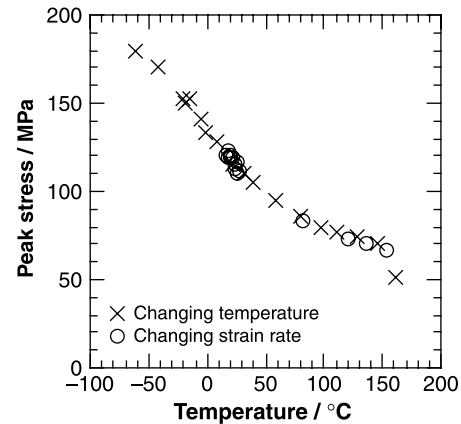


Fig. 8. Comparison of the variation of peak stress with temperature, and the variation of peak stress with strain rate mapped onto temperature.

performed in this study is very good, except at the extremes of temperature, Fig. 9.

3.4.2. DMA data

There are two mappings for these data:

- The glass transition temperature increases by 3.7 °C for every decade increase in strain rate.
- The beta transition temperature increases by 10 °C for every decade increase in strain rate.

These values are consistent with the observation of Swallowe and Lee [20] that the β transition merges with the glass transition at very high strain rates. However, extrapolation of the data for this PC gives the strain rate at which the merge would occur as 10^{30} s^{-1} . The two transitions are therefore distinct at all physical strain rates.

3.4.3. Comparison of compressive and DMA data

Care must be taken when applying mappings to take the glass and β transition temperatures from DMA rates to Hopkinson bar rates, as this involves a large extrapolation: the DMA data were obtained at rates between 6×10^{-4} and $6 \times 10^{-2} \text{ s}^{-1}$, whilst the SHPB experiments were performed at 5500 s^{-1} . However, from the DMA data $T_g = 150 \text{ °C}$ at $6 \times 10^{-4} \text{ s}^{-1}$, and using the relationship of 3.7 °C per decade gives $T_g = 175 \text{ °C}$ at 5500 s^{-1} , which agrees with the SHPB data. The same approach moves the upper end of the beta transition from -50 to $+40 \text{ °C}$, which is equivalent to the temperature at

Table 2
Maximum stresses, in MPa, from Blumenthal et al. [31]

Temperature (°C)	Strain rate (s^{-1})			
	0.001	0.1	5	~2000
55	64			102.4 (@ 2300)
20	72	78	87	117 (@ 2000)
-55	115			234 (@ 3600)
-197	262			

The data were read from stress–strain curves presented in the paper.

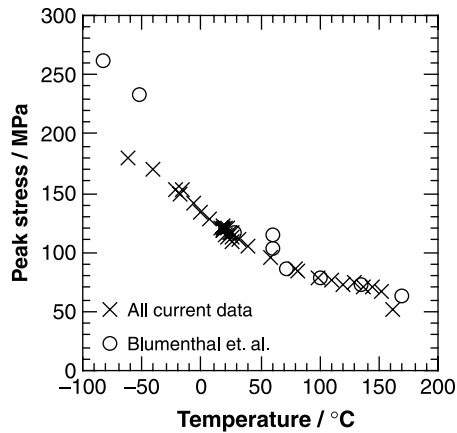


Fig. 9. Comparison of the data from Blumenthal et al. [31] and that from the current research, all mapped to a strain rate of 5500 s^{-1} .

which the bilinear behaviour is observed in the SHPB compressive data.

Since it has been shown that this behaviour in temperature at fixed strain rate is equivalent to that in $\log(\dot{\epsilon})$ at room temperature, the increase in strength at high strain rates can be related to the movement of the β transition at these rates.

In addition, the other end of the β transition is at -100 °C for the 1 Hz DMA data, which is equivalent to -30 °C at the Hopkinson bar rates. This explains the reduction in the gradient of the yield stress– $\log(\dot{\epsilon})$ curves in the two SHPB experiments at -41 and -61 °C , since the Young's modulus is expected to level off at these values.

4. Polyvinylidene difluoride (PVDF)

4.1. Material and specimen preparation

Experiments were performed on Solvay Solef[®] 1012 PVDF. This is described by the manufacturer as a high viscosity homopolymer for processing by extrusion; selected properties from the manufacturer's data sheet are shown in Table 3. The material was provided by the manufacturer as a 3.2 mm thick

Table 3
Selected properties of PVDF

Glass transition temperature	ca. -30 °C
Melting point	174 °C
Number average molecular weight	59×10^3
Average rate of head to head inversions per chain	3.5–4
Density	1.78 g cm^{-3}
Coefficient of linear thermal expansion	$120\text{--}140 \times 10^{-6} \text{ mm}^{-1} \text{ °C}^{-1}$
Tensile modulus	2.4 GPa
Elongation at yield	5–10%
Tensile strength at yield	53–57 MPa
Tensile strength at break	35–50 MPa
Flexural modulus	2.1 GPa
Poisson's ratio	0.35 at 23 °C , 0.5 at 100 °C
Specific heat	$1172 \text{ J kg}^{-1} \text{ K}^{-1}$

At room temperature unless otherwise stated.

moulded sheet. Compression specimens were bored out, and cuboidal DMA specimens were cut, from this sheet. All specimens were annealed using the manufacturers annealing regime. For a specimen of thickness $x \text{ cm}$:

- place in an oven at 100 °C ;
- raise the temperature at $1 \text{ °C per } x \text{ min}$ to 150 °C ;
- hold at 150 °C for $x \text{ h}$; and
- cool to 100 °C at $1 \text{ °C per } x \text{ min}$.

The specimens in these experiments were 3.2 mm thick, and this was used as x . Annealing was performed in the oven of a DMA machine. Annealing tends to make the material slightly creamy in colour.

4.2. Experimental conditions

SHPB experiments were performed at room temperature over strain rates between 1500 and 3600 s^{-1} , and at a nominal strain rate of 2700 s^{-1} over the temperature range -40 to $+150 \text{ °C}$. All of the specimens were 3.2 mm long and 3.9 mm diameter. At 4000 s^{-1} the inertial contribution to the stress for this specimen size is 43 kPa. The specimens were lubricated with paraffin wax. Specimen equilibrium was confirmed by comparing the one and two-wave analyses for specimen stress.

Instron experiments were performed at strain rates between 10^{-4} and 100 s^{-1} at room temperature. DMA analysis was performed at frequencies of 1, 10 and 100 Hz over the temperature range -150 to $+200 \text{ °C}$.

4.3. Results

Fig. 10 shows representative stress–strain curves for PVDF over a range of strain rates at 26 °C . In the Hopkinson bar experiments the specimens exhibit an elastic response until a strain of approximately 0.07 where they begin to yield. There is a peak stress at a strain of approximately 0.11, after which the specimens strain soften. This stress is rate dependent, and ranges from 150 to 170 MPa in these experiments. The Instron data show similar features, at lower stresses, reflecting the lower strain rate. When the temperature is reduced (Fig. 12),

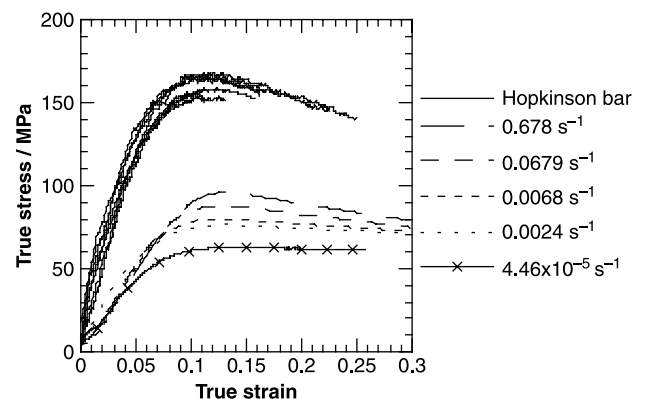


Fig. 10. Stress–strain curves for PVDF at 26 °C . Hopkinson bar strain rates range from 1540 to 3560 s^{-1} .

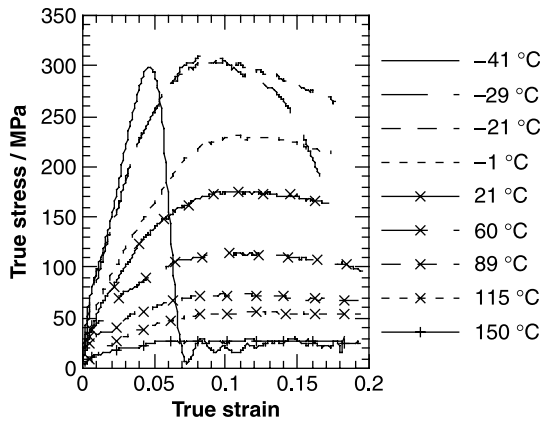


Fig. 11. Hopkinson bar stress–strain curves for PVDF over a range of temperatures at a strain rate of $2700 \pm 150 \text{ s}^{-1}$. At -40°C the response is brittle.

the material becomes stronger. However, the nature of the response remains the same until -25°C , where the strain softening is more dramatic. At -41°C the material was brittle: the manufacturer quotes the glass transition temperature as -30°C , and in the Hopkinson bar experiments it will be higher than this. Increasing the temperature decreases the strength of the material; this also appears to flatten the flow region and move the yield strain to a lower value (Fig. 11).

DMA tests were performed at three frequencies (Fig. 12). The DMA shows the melting temperature, T_m as 179°C , independent of frequency. The rise in modulus around 0°C is due to the glass transition temperature. Further features are described in Section 4.4.

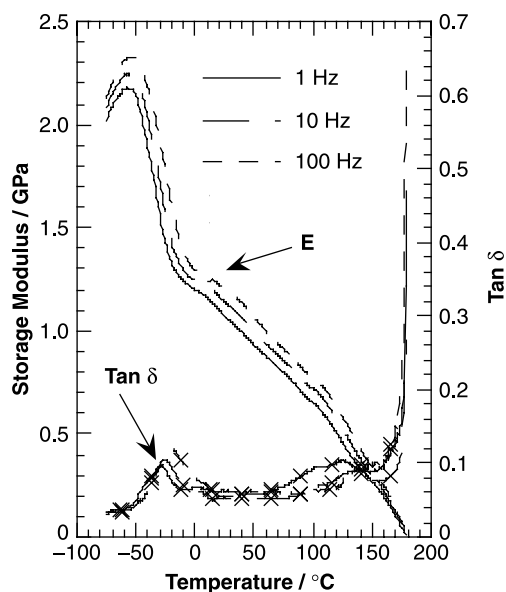


Fig. 12. Storage modulus and $\tan \delta$ for PVDF at frequencies of 1, 10 and 100 Hz, over temperatures from -100 to 180°C in a three-point bend configuration. The strain amplitude was $0.037 \pm 0.0005\%$, the equivalent strain rates are therefore $7.4 \pm 0.1 \times 10^{-4}$, 7.4×10^{-3} and $7.4 \times 10^{-2} \text{ s}^{-1}$. The change in gradient below $\sim -25^\circ\text{C}$ is associated with the glass transition temperature. The melting point is measured as 179°C .

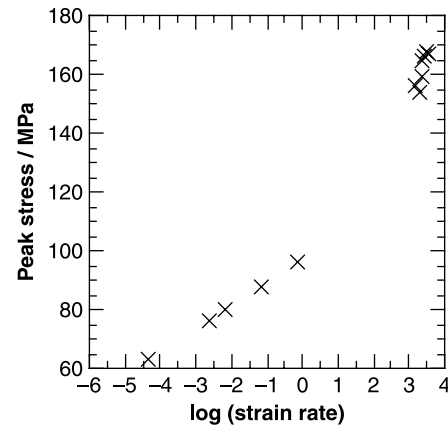


Fig. 13. Plot of maximum stress against strain rate for PVDF at 26°C , showing the two distinct regions in the data.

4.4. Discussion

The maximum stress for each compressive experiment was recorded from the stress–strain curves. The data were then plotted as a function of strain rate at room temperature, and as a function of temperature at 2700 s^{-1} . These plots are shown in Figs. 13 and 14. The data in Fig. 16 show a bilinear dependence of yield stress on strain rate. The temperature dependence is also approximately bilinear. The yield stress rises linearly from zero as the temperature is reduced from T_m . The gradient of the curve increases below 50°C until approximately -20°C , where the maximum stress begins to drop.

In the same manner as the PC data in Section 3, a single parameter mapping was used to convert between temperature and strain rate. In this case, all the data points were mapped to 2850 s^{-1} . The optimum value of A was 17 K (Fig. 15), which is the same as that for the PC data. Whilst the gradient of the mapped Hopkinson bar data at different strain rates agreed with the gradient of the Hopkinson bar data at different temperatures, the mapped Instron data were much higher than the ‘equivalent’ Hopkinson bar data at high temperatures. This is possibly due the fact that, unlike the PC experiments the governing temperature is a melting point rather than a glass transition and therefore does not move with strain rate.

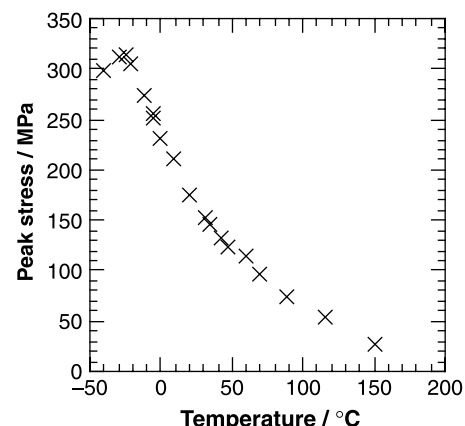


Fig. 14. Plot of maximum stress against temperature for PVDF at $2700 \pm 300 \text{ s}^{-1}$.

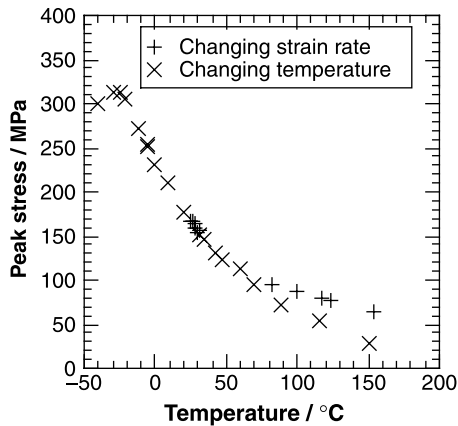


Fig. 15. Comparison of the variation of peak stress with temperature, and the variation of peak stress with strain rate mapped onto temperature.

The DMA data in Fig. 12 show a number of clearly identifiable regions. Between -55 and -10 °C, the modulus decreases with increasing temperature, the gradient of this decrease being the same for all three frequencies. This is the glass transition region. In this region, a 1 decade change in frequency is equivalent to a 5.5 K change in temperature. Between -10 and 0 °C the glass transition region ends, and the modulus now decreases more gradually with increasing temperature. Again, the gradient of the decrease is independent of frequency, and in this region a 1 decade change in frequency is equivalent to a 10 °C change in temperature. This region ends at 100 °C, and unlike the end of the glass transition region, this temperature does not depend on frequency. After this, there is a decrease in modulus to zero at 179 °C, which is associated with the melting point.

From the DMA time–temperature equivalence, the glass transition region at 2700 s^{-1} ranges from -15 to 20 °C, which agrees with the temperatures for the steeper region of the Hopkinson bar data. Therefore, it is concluded that in PVDF the increase in strain rate dependence of the yield stress is due to the glass transition of the polymer moving to room temperature at high strain rates.

5. Discussion

The results presented in this paper examine the mechanical properties of two polymers with different structures: PC—a glassy polymer; and PVDF—a semi-crystalline material. Stress–strain curves were produced for both materials. The data explore the idea of performing experiments over a range of strain rates and temperatures and comparing the data from these using time–temperature superposition. This is shown to be a very successful methodology. In addition, these results were successfully compared to DMA data from the two materials.

The results from experiments performed on PC are in agreement with those described in the literature. The yield stress of the material has a bilinear dependence on $\log(\dot{\epsilon})$ as expected over the range of rates examined. When the temperature is changed, the yield stress has a similar

dependence as the modulus. It was possible to fit a time–temperature equivalence to these data, and map the two sets of experiments onto a temperature dependence at Hopkinson bar rates. The mapping used had only one variable parameter, A , and whilst it might be felt that T_0 and ϵ_0 in Eq. (1) are also parameters, they were later removed by applying the same mapping to data from the literature which examined a ‘two-dimensional’ array of different conditions.

From these data, it was shown that the bilinear dependence of yield stress on $\log(\dot{\epsilon})$ in PC is due to the β transition.

A similar approach was applied to the bilinear behaviour in PVDF. The data again agreed with that in the literature. In this case, the mapping between temperature and strain rate was not able to account for both the high and the low temperature data. This is because the high temperature behaviour is governed by the melting point, which does not move with rate. However, it was shown that for PVDF the bilinear dependence of yield stress on $\log(\dot{\epsilon})$ is due to the glass transition.

However, these data do not explain the drops in flow stress observed by some authors at very high strain rates—in this case by Walley and Field [9] in PC. This may be because the strain rates achieved were not high enough for the drop to occur. In order to investigate this, another of the materials that Walley and Field used was investigated in the Hopkinson bar. Noryl was chosen because the drop in flow stress occurred at a strain rate of 6000 s^{-1} , which is achievable in a traditional SHPB, rather than the miniaturised system used in their research. The dependence of flow stress on $\log(\dot{\epsilon})$ is shown in Fig. 16, and is compared to that of Walley and Field. The drop in flow stress is not observed in the current data.

It is tentatively suggested that the drop in flow stress is specimen size dependence. The size difference between the specimens in the two sets of data in Fig. 16 is in the specimen diameter. Walley and Field chose specimen diameters to keep the aspect ratio of the specimen the same, which was best practice at the time, in the present research the diameter was 5 mm for all experiments. The experiments presented here for PC and PVDF, and in particular the comparison between the

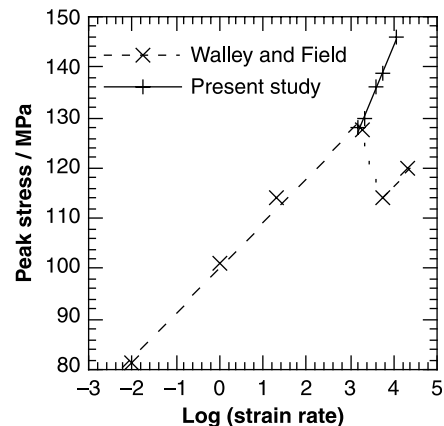


Fig. 16. Comparison of results from Walley and Field [9] and experiments performed as part of the present study. The graph shows flow stress as a function of $\log(\text{strain rate})$. In both cases the errors are of the order 2 MPa or less.

strain rate and temperature dependence, show that this is a reasonable diameter at all the rates used. Calculations also show that inertia is small for polymer specimens of these sizes, and it is known that they can be well-lubricated. However, because expanding ring experiments show this stress drop, this does not seem to be a full explanation, and flow stress drops are an area where further research is required.

6. Conclusions

SHPB experiments have been performed on two different types of polymer: bisphenol-A-polycarbonate (PC)—a glassy polymer; and polyvinylidene difluoride (PVDF)—a semi-crystalline polymer. A methodology has been established for understanding the strain rate dependence of these materials by examining closely the effects of both strain rate and temperature, and mapping between the two.

The increased strain rate dependence of the yield strength of PC at high strain rates is a material property and is due to the movement of the β transition to room temperature at these rates.

The increased strain rate dependence of the yield strength of PVDF at high strain rates is a material property and is due to the movement of the glass transition to room temperature at these rates.

It is now hoped to apply this methodology to other polymers and to establish for each the transitions that are affecting their high strain rate mechanical properties. In addition, further investigations will be performed to establish the cause of flow stress drops observed by some researchers at high rates of strain.

Acknowledgements

The research in this paper was enabled by the kind provision of PVDF specimens and advice by E. Dilley, then of Solvay Fluoropolymers. M. Furze of Bayer also advised on the preparation of PC specimens. The DMA characterisation was performed in the Polymer Characterisation Laboratory in the Department of Materials Science and Metallurgy under the guidance of R. Cornell. The machine was provided by TA Instruments, Crawley. A. Squires annealed the PVDF specimens in the Cavendish Laboratory. Some of the Instron work was performed in the Cavendish with the assistance of D. Williamson, some at Engineering with that of A. Heaver. The authors would also like to thank D. Porter and P. Gould of QinetiQ for their invaluable advice. Finally, C.R. Siviour would like to thank EPSRC, [dstl] and the Worshipful Company of Leathersellers for supporting his research.

Appendix A. Specimen radius and Poisson's ratio

One of the main assumptions when producing true stress—true strain curves for Hopkinson bar specimens is that of volume conservation. This is used to calculate the area of the specimen as a function of time in the experiment, using the measured change in specimen thickness. In order to make more

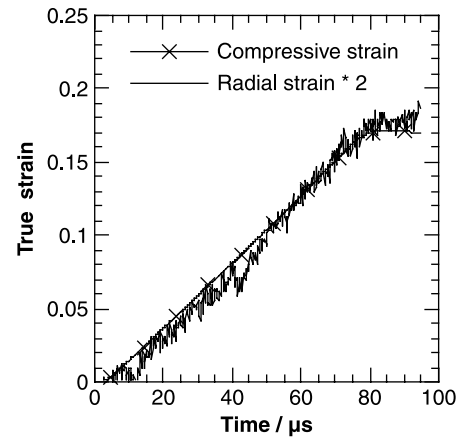


Fig. A1. Comparison of the longitudinal strain calculated using the Hopkinson bar equations, and the radial strain calculated from the line laser, for a specimen of PC. The experiment was performed at 22 °C at 2250 s⁻¹. The radial strain has been doubled for ease of comparison.

accurate measurements, Ramesh and Narasimhan developed the use of a line laser to measure the diameter of a Hopkinson bar specimen continuously through the experiment [32]. The technique is here adopted to calculate the Poisson's ratio of a polycarbonate specimen. Fig. A1 shows a typical result, comparing the longitudinal strain in the specimen calculated from the Hopkinson bar equations to the radial strain calculated from line laser measurements. The Poisson's ratio is the ratio of these two strains, and is shown in Fig. A2, where the stress–strain curve of the material is also presented.

There are a number of important features in Fig. A1. Firstly, the calculation is very noisy at low strains, so it is not possible to measure the low strain value correctly. However, between strains of 0.02 and 0.08 the ratio is 0.45. At yield this jumps to 0.5, which is consistent with the idea of yield being equivalent to a glass transition, and being the point at which irreversible plastic deformation begins [33]. In addition, it is in agreement with the result of Chou, that the bulk of the temperature rise in a deforming polymer occurs after the glass yield [1]. Because the Poisson's ratio is derived using true strains it refers both to

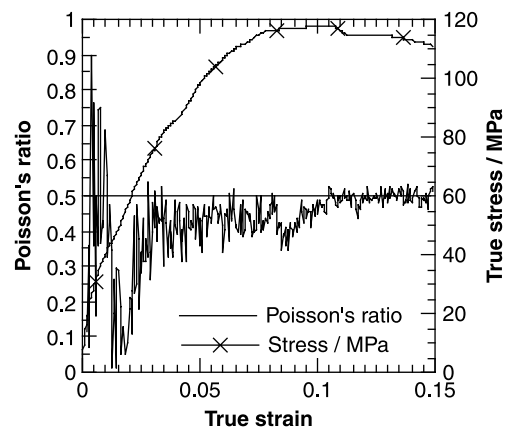


Fig. A2. The evolution of Poisson's ratio with strain in the specimen of PC from Fig. A1. The stress–strain curve for this specimen is also shown, and comparison of the two curves shows the jump in Poisson's ratio as the specimen yields.

incremental increases in strain and the overall strain during the experiment. Therefore, a jump from 0.45 to 0.5 shows that the specimen initially undergoes a decrease in volume, but then returns to its original volume at yield. This would involve the rapid release of the built up strain energy, which must become heat.

References

- [1] Chou SC, Robertson KD, Rainey JH. *Exp Mech* 1973;13:422–32.
- [2] Briscoe BJ, Hutchings IM. *Polymer* 1976;17:1099–102.
- [3] Kukureka SN, Hutchings IM. Measurement of the mechanical properties of polymers at high strain rates by Taylor impact. In: Blazynski TZ, editor. Proceedings of the 7th international conference on high energy rate fabrication. Leeds: University of Leeds; 1981. p. 29–38.
- [4] Briscoe BJ, Nosker RW. *Wear* 1984;95:241–62.
- [5] Briscoe BJ, Nosker RW. *Polym Commun* 1985;26:307–8.
- [6] Gorham DA. *J Phys D: Appl Phys* 1991;24:1489–92.
- [7] Walley SM, Field JE, Pope PH, Safford NA. *Philos Trans R Soc London, Ser A* 1989;328:1–33.
- [8] Walley SM, Field JE, Pope PH, Safford NA. *J Phys III France* 1991;1: 1889–925.
- [9] Walley SM, Field JE. *DYMAT J* 1994;1:211–28.
- [10] Rietsch F, Bouette B. *Eur Polym J* 1990;26:1071–5.
- [11] Bisilliat ML, Gary G, Klepaczko JR, Billon N. Compression test on a polycarbonate over a wide range of strain rates. Proceedings of the 10th international conference on deformation, yield and fracture of polymers. London: The Institute of Materials; 1997 p. 203–206.
- [12] Al-Maliky N, Fernandez JO, Parry DJ, Swallowe GM. *J Mater Sci Lett* 1998;17:1141–3.
- [13] Hamdan S, Swallowe GM. *J Polym Sci B, Polym Phys* 1996;34:699–705.
- [14] Hamdan S, Swallowe GM. *J Mater Sci* 1996;31:1415–23.
- [15] Al-Maliky NS, Parry DJ. *Meas Sci Technol* 1996;7:746–52.
- [16] Dioh NN, Leever PS, Williams JG. *Polymer* 1993;34:4230–4.
- [17] Dioh NN, Ivankovic A, Leever PS, Williams JG. *J Phys IV France Colloq C8 (DYMAT 94)* 1994;4:119–24.
- [18] Swallowe GM, Fernandez JO. *J Phys IV France Pr 9 (DYMAT 2000)* 2000;10:311–6.
- [19] Swallowe GM, Fernandez JO, Hamdan S. *J Phys IV France Colloq C3 (EURODYMAT 97)* 1997;7:453–8.
- [20] Swallowe GM, Lee SF. *J Phys IV France* 2003;110:33–8.
- [21] Bauwens-Crowet C. *J Mater Sci* 1973;8:968–79.
- [22] Bauwens-Crowet C, Bauwens JC, Homès G. *J Mater Sci* 1972;7:176–83.
- [23] Bauwens JC. *J Mater Sci* 1972;7:577–84.
- [24] Rittel D. *Mech Mater* 1999;31:131–9.
- [25] Gray III GT, Blumenthal WR. Split-Hopkinson pressure bar testing of soft materials. In: Kuhn H, Medlin D, editors. *ASM handbook. Mechanical testing and evaluation*, vol. 8. Materials Park, OH: ASM International; 2000. p. 488–96.
- [26] Gray III GT. Classic split-Hopkinson pressure bar testing. In: Kuhn H, Medlin D, editors. *ASM handbook. Mechanical testing and evaluation*, vol. 8. Materials Park, OH: ASM International; 2000. p. 462–76.
- [27] Gorham DA. *J Phys D, Appl Phys* 1989;22:1888–93.
- [28] Williams ML, Landel RF, Ferry JD. *J Am Chem Soc* 1955;77:3701–7.
- [29] Trautmann A, Siviour CR, Walley SM, Field JE. *Int J Impact Eng* 2005; 31:523–44.
- [30] Hutchinson JM. Relaxation processes and physical aging. In: Hawaed RN, Young RJ, editors. *The physics of glassy polymers*. London: Chapman & Hall; 1997. p. 85–146.
- [31] Blumenthal WR, Cady CM, Lopez MF, Gray III GT, Idar DJ. Influence of temperature and strain rate on the compressive behavior of PMMA and polycarbonate polymers. In: Furnish MD, Thadani NN, Horie Y, editors. *Shock compression of condensed matter—2001*. Melville, NY: American Institute of Physics; 2002. p. 665–8.
- [32] Ramesh KT, Narasimhan S. *Int J Solids Struct* 1996;33:3723–38.
- [33] Bowden PB. The yield behaviour of glassy polymers. In: Haward RN, editor. *The physics of glassy polymers*. 1st ed.. London: Applied Science; 1973. p. 279–339.